Solid–Liquid Interface

DOI: 10.1002/anie.201203910

First In Situ Observation of the $LiCoO_2$ Electrode/Electrolyte Interface by Total-Reflection X-ray Absorption Spectroscopy**

Daiko Takamatsu, Yukinori Koyama, Yuki Orikasa, Shinichiro Mori, Takayuki Nakatsutsumi, Tatsumi Hirano, Hajime Tanida, Hajime Arai, Yoshiharu Uchimoto, and Zempachi Ogumi*

Rechargeable lithium-ion batteries (LIBs) are widely used as electrical energy storage devices for technologies such as portable electronics and electric and hybrid vehicles, and they are considered to be serious power storage candidates for smart-grid electricity systems.[1] Traditionally, research in the field has focused on battery improvement through a selective use of new or existing materials for positive and negative electrodes, as the bulk properties of electrodes primarily limit charge capacity and power.[2] However, the durability of LIBs is largely rooted in side reactions that occur at the electrode/electrolyte interface, especially those at the positive electrode.[3] Thus, controlling the chemical stability of any electrode material with respect to the operating liquid electrolyte medium, which requires a control of the electrode/electrolyte interface through surface chemistry, is as important as designing new materials. The scale of such an interfacial region is speculated to be on the order of a few nanometers, which shall be deemed as approximately the Debye length.[4] This scale indicates that structural and chemical information should be tracked with a resolution of a few nanometers to reveal the phenomena of the electrode/electrolyte interface. Previous research has focused on a detailed examination of the interfacial reactions at the positive electrode surface by using methods such as X-ray photoelectron spectroscopy (XPS) and surface X-ray diffraction (SXRD).[5] However, characterization of the electrode surface at the nanoscale under conditions of an operating battery remains insufficient because of the lack of suitable observation techniques. A proposed degradation mechanism for electrodes has been extrapolated from indirect information obtained from analysis of disassembled, deteriorated electrodes.

To obtain concise and meaningful surface data, a technique that enables high-resolution analysis of chemical information at the solid electrode surface is required. X-ray absorption spectroscopy (XAS), which makes it possible to identify the electronic and local structures of a certain atom,[6] is a potent and versatile technique to resolve the chemical states of a lithium-ion electrode material independently of its crystallinity. To extract information about the interfacial phenomena by XAS, total-reflection fluorescence XAS (TRF-XAS), which integrates the fluorescence yield obtained under total reflection,[7] can be applied. A recent study has shown that polycrystalline thin films are preferred relative to epitaxial thin films (that are strongly influenced by the substrate) to simulate the conditions of applied composite electrodes.[8] We herein use polycrystalline $LiCoO_2$ thin films prepared by pulsed laser deposition (PLD) as the model electrodes; these electrodes are flat at the nanoscale and have structural properties similar to those of the applied composite electrode (see section S1 in the Supporting Information).

Figure 1 shows the charge/discharge cycle dependencies of cyclic voltammograms (CVs) and electrochemical impedance spectra (EIS) of the $LiCoO_2$ thin films used in this study (see section S1 in the Supporting Information). Typical CVs

[*] Dr. D. Takamatsu, Prof. Dr. Y. Koyama, Prof. Dr. H. Tanida, Prof. Dr. H. Arai, Prof. Dr. Z. Ogumi
Office of Society-Academia Collaboration for Innovation
Kyoto University, Uji-shi, Kyoto 611-0011 (Japan)
E-mail: takamatsudik@rising.saci.kyoto-u.ac.jp
Dr. Y. Orikasa, S. Mori, T. Nakatsutsumi, Prof. Dr. Y. Uchimoto
Graduate School of Human and Environmental Studies
Kyoto University, Sakyo-ku, Kyoto 606-8501 (Japan)
T. Hirano
Hitachi Research Laboratory, Hitachi, Ltd.
Hitachi-shi, Ibaraki 319-1292 (Japan)

[**] This work was supported by the "Research and Development Initiative for Scientific Innovation of New Generation Battery (RISING project)" of the New Energy and Industrial Technology Development Organization (NEDO; Japan). The synchrotron radiation experiments were performed with the approval of the Japan Synchrotron Radiation Research Institute (JASRI; proposal numbers 2009B1027, 2010A1015, 2010A1016, 2010B1029, 2011A1012, 2011B1022, 2011B1023, and 2011B1037).

Supporting information for this article is available on the WWW under http://dx.doi.org/10.1002/anie.201203910.

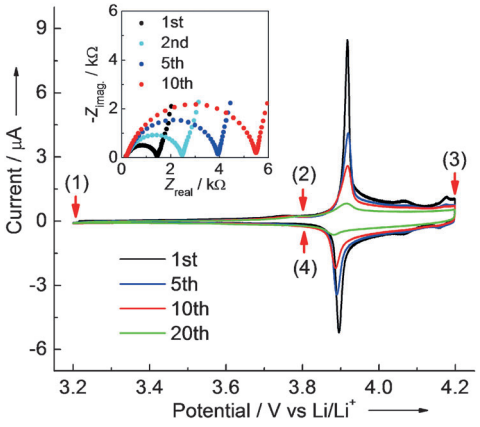

Figure 1. Cycling behavior of polycrystalline $LiCoO_2$ thin-film electrodes. A Cyclic voltammogram is shown and in the inset electrochemical impedance spectra obtained at 4.0 V (versus Li/Li^+) are displayed. The potential sweep rate was set to 0.1 $mV s^{-1}$ between 3.2–4.2 V (versus Li/Li^+). Arrows marked with (1)–(4) denote the points, at which the X-ray absorption spectra shown in Figure 4 were measured.

of $LiCoO_2$ were observed that were characterized by three sets of well-defined current peaks: a conspicuous sharp peak at about 3.9 V (versus Li/Li^+) and small inconspicuous peaks at 4.06 and 4.18 V.[9] With an increasing number of electrochemical cycles, the peak intensity in the CVs gradually became smaller and the peak separation became larger. The charge-transfer resistance in the electrochemical impedance spectra increased gradually with the number of electrochemical cycles (inset in Figure 1). These results indicated that the reversibility of the polycrystalline $LiCoO_2$ thin films gradually decreased with increasing charge/discharge cycles, even if the cycles were limited to an upper voltage of 4.2 V, which corresponds to the nominal composition range of $0 \le x \le 0.55$ in $Li_{1-x}CoO_2$.[10] The cycle durability of the thin films is more pronounced than the durability of the composite electrodes in applied LIBs because the volume ratio of the electrode surface/electrolyte solution is enhanced in the thin films relative to the composite electrodes.

The reflective index of the X-ray is slightly smaller than unity. Therefore, a highly collimated X-ray beam applied to a flat surface at an angle smaller than the critical angle is totally reflected.[11] Such a beam penetrates the sample to a depth of only a few nanometers. Under this condition, only atoms at the surface of the electrode are excited and only the surface information is extracted. The critical angle and penetration depth of $LiCoO_2$ was calculated (see section S2 in the Supporting Information). In these studies, the theoretical and experimental wavelength of the incident X-ray was 1.61 Å (7.7 keV), which corresponds to a Co *K*-edge fluorescence X-ray used for XAS measurements. Figure 2a shows the calculated incident angle dependence of the X-ray intensity and the penetration depth at which the X-ray intensity attenuates to $1/e$ in $LiCoO_2$. The calculated critical angle of total reflection (θ_{TR}) of $LiCoO_2$ was 0.28° and the corresponding penetration depth was 6.8 nm. Figure 2b (electrode only) shows the glancing-angle dependence of the intensity of the Co *K*-edge fluorescence X-rays from a $LiCoO_2$ thin film. A distinctive increase in the fluorescence intensity was observed at approximately 0.3° (Figure 2b), which was in good agreement with the calculated result shown in Figure 2a. The penetration depth at each incident angle can be obtained by comparing the results of Figure 3a and b. When the incident angle was set at 0.2° (an angle smaller than θ_{TR}), the penetration depth was estimated to be about 3 nm (denoted as "surface" in Figure 2b). The bulk information was obtained by setting the incident angle at 2.2°; under this condition, the penetration depth was estimated to be greater than 100 nm. As the thickness of the $LiCoO_2$ film used in this study was approximately 50 nm, information about the whole film can be obtained (denoted as "bulk material" in Figure 2b).

This method was then applied to the $LiCoO_2$ surface immersed in a liquid electrolyte. As the reflective index of the X-ray in a liquid electrolyte is also slightly smaller than unity, θ_{TR} is either the same or smaller compared to θ_{TR} of the electrode only. The dependence of the incident angle of the fluorescence X-ray on the $LiCoO_2$ thin film was examined in a spectro-electrochemical cell, as schematically shown in Figure 2c. The cell was composed of a $LiCoO_2$ film on a platinum (Pt) substrate as the working electrode (WE), a lithium-metal sheet as the counter electrode (CE), 1 mol L $LiClO_4$ in a 1:1 volumetric mixture of ethylene carbonate (EC) and diethyl carbonate (DEC) as electrolyte, and a microporous membrane (CELGARD®3501) as a separator. The cell was sealed from the atmosphere and the free space of the cell was filled with flowing helium gas. The intensity of the fluorescence X-rays was remarkably decreased by absorption through the electrolyte, separator, and lithium metal (shown as "in situ cell" in Figure 2b). However, because of the high permeability of synchrotron X-rays, the electrode surface is distinguishable even though the spectro-electrochemical cell is used. These results show that differentiation of surface and bulk material at the electrode/electrolyte interface can be realized by using the total-reflection method.

Figure 3 shows the normalized Co *K*-edge TRF-XAS (XANES = X-ray absorption near-edge structure) spectra obtained from the bulk material and the surface before and after electrolyte soaking (see section S3 in the Supporting Information). The XANES spectra of the bulk material were unchanged by electrolyte soaking. In contrast, the surface XANES spectra were significantly changed by electrolyte soaking. The energy level shifted toward lower energy in the surface XANES spectra, which was attributable to a reduction of the Co ions at the surface of the $LiCoO_2$ electrode by contact with the electrolyte. As the XANES spectra of the bulk material were unchanged by electrolyte soaking, the reduction of the Co ions must have occurred within a depth of a few nanometers from the surface of the electrode. Such

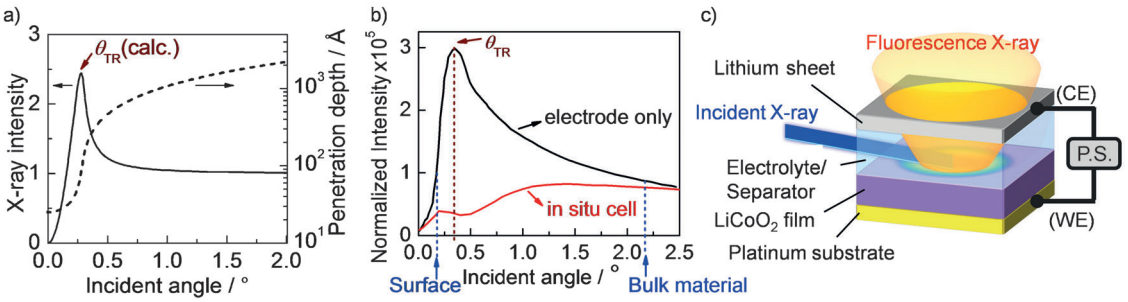

Figure 2. a) Calculated X-ray intensity and penetration depth of the 7.7 keV incident X-ray to $LiCoO_2$. The X-ray intensity was evaluated as a square of the transmission coefficient. b) Incident X-ray angle dependence of the Co fluorescence from $LiCoO_2$/Pt, obtained before electrolyte soaking (black) and after electrolyte soaking (red). c) The spectro-electrochemical cell used for in situ TRF-XAS measurements (P.S. = potentiostat).

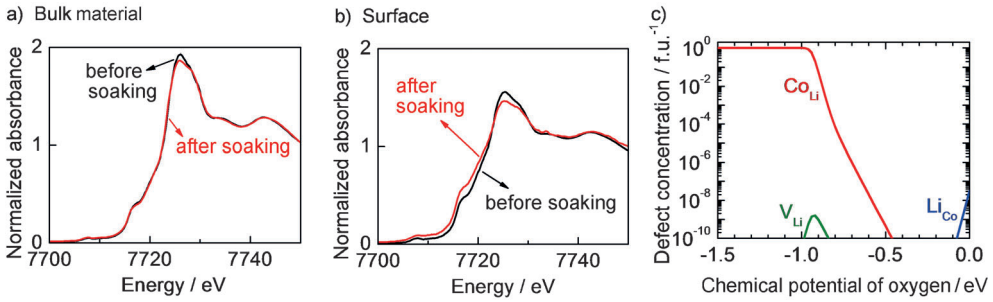

Figure 3. Surface changes resulting from contact with liquid electrolyte. a) Co *K*-edge TRF-XANES spectra of the bulk $LiCoO_2$ film, and b) spectra of the surface before (black) and after (red) electrolyte soaking. c) DFT calculation of the equilibrium defect concentrations in $LiCoO_2$ as a function of the atomic chemical potential of environmental oxygen (f.u.$^{-1}$ = (formula unit)$^{-1}$).

nanoscale phenomena cannot be obtained by conventional techniques for studying bulk materials.

The reduction of Co at the electrode surface was confirmed by theoretical calculations. Equilibrium defect concentrations in $LiCoO_2$ under reducing chemical conditions at room temperature were estimated by density functional theory (DFT) calculations, and the results are shown in Figure 3c. As the chemical potential for oxygen decreased (under stronger reducing conditions), the concentration of the antisite Co ion at the Li site (Co_{Li}) increased considerably. The antisite Co ion was in the divalent state, and the excess charge was compensated with another divalent Co ion at the regular site. The concentration of the antisite defect Co_{Li} was so high at a oxygen chemical potential of −1 eV or less that $LiCoO_2$ was no longer stable. The chemical potential for oxygen in an organic electrolyte such as EC is deemed to be less than −2 eV. The equilibrium can be achieved only at the surface to a depth of a few nanometers because the diffusion of cobalt and oxygen at room temperature is slow. The DFT calculations suggest that Co is reduced at the surface when the electrode sample is immersed in the organic electrolyte. The suggested surface reduction reaction can be formulated as given in Equation (1),

$$LiCoO_2 + S \rightarrow Co_{Li}^{\bullet} + e' + Li_2O + SO \quad (1)$$

where S and SO are the electrolyte solution component and the corresponding oxidized product, respectively. $Co_{Li}^{\bullet}$ is the divalent Co that replaces Li, and e' is the divalent Co at the regular Co site. The Li-containing product is denoted as Li_2O in the above-mentioned reaction (1) for simplicity, but it would react with the oxidized electrolyte components (SO) to form Li_2CO_3 or lithium alkyl carbonate. The surface extended X-ray absorption fine structure (EXAFS) spectra showed an increase in lattice distortion, which is described by the Debye–Waller (DW) factor, and/or a decrease of the coordination numbers by electrolyte soaking, whereas the bulk material retains a layered six-coordinated CoO_6 octahedral structure (see section S4 in the Supporting Information).

The XAS spectra and DFT calculations suggest that the local environment of the Co ions at the surface of the electrode drastically changed by electrolyte soaking as compared with the bulk $LiCoO_2$ material. Herein we show that the electronic and local structural changes occurring at the nanoscale of the electrode/electrolyte interface can indeed be detected by using in situ TRF-XAS.

Figure 4a and b shows the bulk material and surface Co *K*-edge XANES spectra obtained at each state of charge [marked with arrows (1) to (4) in Figure 1] at controlled potentials. The XANES spectra of the bulk material shifted continuously towards higher (Co oxidation) and lower (Co reduction) energy levels as electrochemical charging and discharging proceeded, respectively. Extraction of lithium from $LiCoO_2$ is known to provoke both an increase of the pre-edge peak and a shift to a higher energy of the main maximum in the Co-*K* edge XANES spectra, and our results (Figure 4a) are consistent with those reported in the literature.[12] Herein, we focused on surface-specific phenomena and used the energy shift of the XANES spectra to identify the oxidation state of the Co species. Figure 4c and d shows the absorption energy at the normalized intensity of 0.5 in the XANES spectra during the course of the electrochemical experiments. In the case of the bulk material, the energy returns back to the original position after charge and discharge processes, suggesting that the $LiCoO_2$ bulk material keeps its layered structure and shows a good electrochemical reversibility. As the energy levels of the surface XANES spectra also changed during the charge/discharge processes, it is suggested that the surface Co species are still electrochemically active. However, the behavior at the surface is essentially irreversible, in contrast to the good reversibility in the bulk material. It appears that the surface Co^{2+} species formed during the electrolyte-soaking process are oxidized during the charging process, but the reduction is insufficient. A hypothesis is that $Li_xCo_{1-x}O$ formed at the surface is oxidized to Co_3O_4 or other species during charging and subsequently cannot be reduced during discharging. These Co^{3+} species, formed during the charging process, may be partially reduced by electrolyte solvents. The electrically conductive (and perhaps electrochemically active) surface Co^{2+} species appears to be responsible for the slow but important loss of durability in these electrodes. If the surface is electrochemically active and is continuously reduced during immersion in the electrolyte, the deterioration can propagate. The observed Co reduction at the nanoscale would be an initial deterioration that starts at the surface of $LiCoO_2$ even at the first cycle.

Figure 4e displays the proposed deterioration mechanism that occurs at the electrode/electrolyte interface in LIBs. The Co ion (Co^{3+}) at the surface of $LiCoO_2$ is reduced to a Co^{2+} ion by organic electrolyte soaking. The local structure is distorted when the Co^{3+} ion reacts with the electrolyte and is reduced to Co^{2+}, and this distortion propagates during the consecutive charge/discharge processes. Accordingly, the

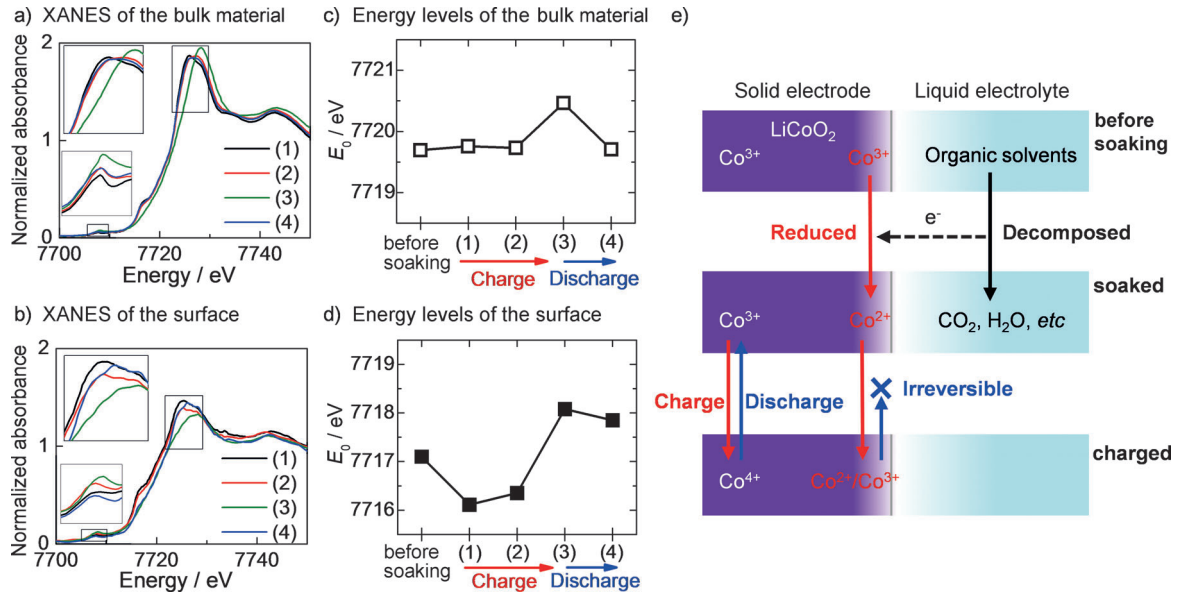

Figure 4. a)–d) Co *K*-edge XANES spectra of the $LiCoO_2$ film measured at points (1)–(4) in Figure 1 by applying a voltage and measuring the corresponding absorption energy levels of the bulk material (a, c) and the surface (b, d), respectively. e) The proposed reaction of the initial degradation that occurs at the electrode/electrolyte nano-interface.

initial deterioration that starts at the surface of $LiCoO_2$ on electrolyte immersion can lead to a loss of durability that occurs during longer time scales. The analyses suggest that the initial deterioration (the reduction of Co ions at the nano-scale) also occurs in the composite electrodes of applied LIBs. It is important to suppress this initial deterioration to prolong the cycle performance of LIBs. Surface modification of electrodes with oxide layers and/or electrolyte additives to form electronic insulating films on the electrode surface can be one of the effective ways to prevent this deterioration.

In conclusion, the chemical state of Co ions at the surface (at a depth of about 3 nm) and in the bulk material (at a depth greater than 100 nm) of the polycrystalline $LiCoO_2$ thin-film electrode were comparatively studied by in situ TRF-XAS. Direct observations of the electronic and local structures and their changes at the electrode/electrolyte interface of the $LiCoO_2$ system during charge/discharge processes were successfully established. A reduction of Co ions at the surface of the $LiCoO_2$ electrode that is in contact with organic electrolyte solutions occured. The irreversible behavior was observed at the surface of $LiCoO_2$ during the first charge/discharge process. This Co reduction that occurs at the nano-interface of the electrode/electrolyte can be the initial deterioration of LIBs.

Experimental Section

A 50 nm thick film of $LiCoO_2$ was deposited at 600 °C for 30 min on a mechanically polished platinum polycrystalline substrate by PLD (see the Supporting Information). TRF-XAS measurements were performed at BL01B1 and BL37XU at SPring-8 (JASRI, Japan) with a solid-state detector (19 elements SSD). Electrochemical lithium (de-)intercalation was performed by controlling the potential using a potentiostat. After stabilizing the cell potential (i.e. after the cell reached equilibrium conditions), TRF-XAS measurements were performed on both surface and bulk material, alternatively. After each TRF-XAS measurement, the cell potential changed until it attained a fixed value for the next potentiostatic measurement.

DFT calculations on the defects in $LiCoO_2$ were performed using the plane-wave basis projected-augmented-wave (PAW) method implemented in the VASP code[13] with the generalized gradient approximation, including the Hubbard U correlation[14] (GGA + U, $U = 5$ eV). Supercells consisting of 144 atoms with an additional single defect were used. Li, Co, and O vacancies, antisite cations, and interstitial cations were considered as the possible defects. The plane-wave basis set was determined by a cutoff energy of 500 eV. Integration in the reciprocal space was performed by the Gaussian smearing technique with a smearing parameter of $\sigma = 0.1$ eV using a $2 \times 2 \times 1$ mesh. The theoretical scheme and assumptions on the chemical conditions to calculate the defect concentrations is described in section S5 in the Supporting Information.

Received: May 21, 2012
Revised: September 12, 2012
Published online: October 12, 2012

Keywords: density functional calculations · electrochemistry · lithium batteries · solid–liquid interface · X-ray absorption spectroscopy

[1] a) J. M. Tarascon, M. Armand, *Nature* **2001**, *414*, 359–367; b) M. Armand, J. M. Tarascon, *Nature* **2008**, *451*, 652–657.
[2] a) J. M. Goodenough, Y. Kim, *Chem. Mater.* **2010**, *22*, 587–603; b) B. Scrosati, J. Garche, *J. Power Sources* **2010**, *195*, 2419–2430; c) B. L. Ellis, K. T. Lee, L. F. Nazar, *Chem. Mater.* **2010**, *22*, 691–714.
[3] a) K. Edström, T. Gustafsson, J. O. Thomas, *Electrochim. Acta* **2004**, *50*, 397–403; b) D. Aurbach, B. Markovsky, G. Salitra, E. Markecich, Y. Talyossef, M. Koltypin, L. Nazar, B. Ellis, D. Kovacheva, *J. Power Sources* **2007**, *165*, 491–499.
[4] A. J. Bard, L. R. Faulkner, *Electrochemical Methods: Fundamentals and Applications*, 2nd ed., Wiley, New York, **2001**.
[5] a) M. Shikano, H. Kobayashi, S. Koike, H. Sakaebe, E. Ikenaga, K. Kobayashi, K. Tatsumi, *J. Power Sources* **2007**, *174*, 795–799;

b) R. Dedryvère, L. Gireaud, S. Grugeon, S. Laruelle, J. M. Tarascon, D. Gonbeau, *J. Phys. Chem. B* **2005**, *109*, 15868 – 15875; c) A. M. Andersson, D. P. Abraham, R. Haasch, S. MacLaren, J. Liu, K. Amine, *J. Electrochem. Soc.* **2002**, *149*, A1358 – A1369; d) J. Song, S. Jacke, G. Cherkashinin, S. Schmid, Q. Dong, R. Hausbrand, W. Jaegermann, *Electrochem. Solid-State Lett.* **2011**, *14*, A189 – A191; e) M. Hirayama, H. Ido, K. Kim, W. Cho, K. Tamura, J. Mizuki, R. Kanno, *J. Am. Chem. Soc.* **2010**, *132*, 15268 – 15276.

[6] D. C. Koningsberger, R. Prins, *X-ray absorption*, Wiley, New York, **1988**.

[7] G. Martens, P. Rabe, *Phys. Status Solidi A* **1980**, *58*, 415 – 424.

[8] D. Takamatsu, T. Nakatsutsumi, S. Mori, Y. Orikasa, M. Mogi, H. Yamashige, K. Sato, T. Fujimoto, Y. Takanashi, H. Murayama, M. Oishi, H. Tanida, T. Uruga, H. Arai, Y. Uchimoto, Z. Ogumi, *J. Phys. Chem. Lett.* **2011**, *2*, 2511 – 2514.

[9] a) Y. Iriyama, M. Inaba, T. Abe, Z. Ogumi, *J. Power Sources* **2001**, *94*, 175 – 182; b) W. S. Yoon, K. B. Kin, M. G. Kim, M. K. Lee, H. J. Shin, J. S. Lee, C. H. Yo, *J. Phys. Chem. B* **2002**, *106*, 2526 – 2532.

[10] a) H. Arai, M. Hayashi, *Encycl. Electrochemical Power Sources* **2009**, *5*, 258 – 263; b) Z. Chen, J. R. Dahn, *Electrochim. Acta* **2004**, *49*, 1079 – 1090.

[11] H. Saisho, Y. Gohshi, *Applications of synchrotron radiation to materials analysis*, Elsevier Science B.V., Amsterdam, **1996**.

[12] a) I. Nakai, K. Takahashi, Y. Shiraishi, T. Nakagome, F. Nishikawa, *J. Solid State Chem.* **1998**, *140*, 145 – 148; b) W. S. Yoon, K. K. Lee, K. B. Kim, *J. Electrochem. Soc.* **2000**, *147*, 2023 – 2028.

[13] a) G. Kresse, J. Furthmüller, *Phys. Rev. B* **1996**, *54*, 11169 – 11186; b) P. E. Blöchl, *Phys. Rev. B* **1994**, *50*, 17953 – 17979; c) G. Kresse, D. Joubert, *Phys. Rev. B* **1999**, *59*, 1758 – 1775.

[14] a) J. P. Perdew, K. Burke, M. Ernzerhof, *Phys. Rev. Lett.* **1996**, *77*, 3865 – 3868; b) S. L. Dudarev, G. A. Botton, S. Y. Savrasove, C. J. Humphreys, A. P. Sutton, *Phys. Rev. B* **1998**, *57*, 1505 – 1509.

